Weldability of Fe-36%Ni Alloy (Report III)†

—Dynamic Observation of Reheat Hot Crack and Evaluation of Hot Ductility of Reheated Weld Metal—

Yue-Chang ZHANG*, Hiroji NAKAGAWA** and Fukuhisa MATSUDA***

Abstract

This study has been planned to analyze the behavior of reheat hot cracking in the weld metal of Invar by means of the direct observation technique (MISO) coupled with the Cross-bead tensile hot cracking test. Moreover, hot ductility test was applied to study the characteristic of ductility trough causing the reheat hot crack. Main conclusions obtained are as follows: 1) The initiation of the reheat hot crack occurred at about 850°C and the propagation did in the temperature range from about 600 to 1000°C. 2) Increase in crosshead speed causes high ductility and different fracture mode from that in the weld cracking test. 3) There is a good correlation between the total crack length in the weld cracking test and the characteristic of ductility curve in the hot ductility test. 4) Brittleness temperature range and minimum ductility which secure crack free welding in fabrication of membrane-type LNG tanks were evaluated.

KEY WORDS: (Hot Cracking) (GTA Welding) (Controlled Expansion Alloys) (Containers)

1. Introduction

In the previous papers[1,2], microstructural and fractographic features of reheat hot crack in weld metal of Fe-36%Ni alloy (Invar), harmful elements causing the crack, and secure chemical compositions insusceptible to the crack in actual fabrication were studied. The mechanism of the reheat hot crack, however, has not been clear yet. It was shown[1,2] that this reheat crack is not liquation crack although sulphur is one of the harmful elements. Moreover there is no possibility that intergranular carbides cause the crack as seen in the ductility-dip crack in the weld metal of fully austenitic stainless steel[3], because no carbide former element is included. Although proper chemical compositions to secure crack-free welding in fabrication has been established[2], it should be necessary to reveal the mechanism for the sake of the prevention of similar type of the reheat crack which will occur in other new alloys in future.

Recently, the authors developed the MISO technique[4,5], which enables dynamic photographing of initiation and propagation of cracking during welding through microscope and also strain measurement by the film analysis. Therefore, firstly this study has been planned to analyze the dynamic behavior of the reheat hot crack in the weld metal of Invar reheated by the following welding pass. Consequently, the temperature of the initiation and propagation of the hot cracking has been made clear.

Then, hot ductility test has been planned to compare the cracking temperature range measured by the MISO technique with the temperature range of the ductility trough in the test, including the effect of crosshead speed on the ductility, in order to study the applicability of the hot ductility test which is considered to be more suitable to reveal the mechanism. Moreover, the correlation between the crack tendency in the Cross-bead tensile hot cracking test in the previous paper[2] and the characteristics of hot ductility has been studied for the sake of simple evaluation of hot crack susceptibility.

2. Experimental Procedures

2.1 Materials used

Thin sheets of eight tentative Fe-36%Ni alloys (Invar)

† Received on April 30, 1985
* Foreign Researcher (Shanghai Jiao Tong Univ.)
** Research Instructor
*** Professor

Transactions of JWRI is published by Welding Research Institute of Osaka University, Ibaraki, Osaka 567, Japan

were used, and their chemical compositions are shown in **Table 1**. Their item numbers are the same as those in the previous paper[2]. The total crack length (L) measured with the Cross-bead tensile hot cracking test[1,2] is also given in Table 1. It is understood that the materials of high, medium and low susceptibilities to the reheat hot crack were provided. The thickness of specimens used in the Cross-bead tensile hot cracking test was 1.5 mm, and that used in the hot ductility test was 3 mm. They were solution-treated at 1100°C.

Table 1 Chemical compositions of materials used

Item No.	Composition (wt.%)									L*
	C	Si	Mn	P	S	N	O	Al	Ni	
1	0.031	0.20	0.50	0.002	0.0011	0.0008	0.0034	0.009	36.25	0.7
3	0.029	0.19	0.37	0.005	0.0025	0.0013	0.0040	0.003	36.28	5.8
4	0.025	0.17	0.35	0.004	0.0004	0.0007	0.0018	0.008	35.81	2.9
7	0.034	0.18	0.35	0.002	0.0005	0.0010	0.0016	0.002	35.93	0.2
9	0.017	0.19	0.36	0.001	0.005	0.0017	0.0036	0.001	36.20	48.5
12	0.033	0.19	0.35	0.003	0.005	0.0035	0.0021	0.001	36.05	35.4
14	0.035	0.51	1.04	0.0005	0.001	0.0008	0.0014	0.004	35.8	11.1
18	0.049	0.49	1.01	0.012	0.0010	0.0086	0.0069	0.001	35.8	25.5

* L: Total crack length in Cross-bead cracking test

2.2 Dynamic analysis of cracking behavior

The direct observation technique MISO[4] was combined with the Cross-bead tensile hot cracking test[1] to analyze the initiation and propagation behaviors of the reheat hot cracking during welding. Its procedure is as follows: First pass GTA welding was done prior to test welding, and then the specimen machined as shown in **Fig. 1** was set to a horizontal tensile cracking tester. Load

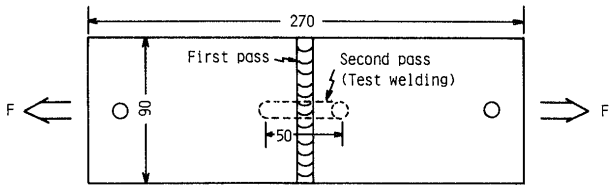

Fig. 1 Specimen configuration used for the Cross-bead tensile hot cracking test coupled with the MISO technique.

(F) was applied perpendicularly to the first pass so that the average stress of the specimen might be 15 kgf/mm^2. Then the test welding, namely, the second pass GTA welding was done perpendicularly to the first pass, whereas tensile deformation in crosshead speed (C.H.S.) of 0.13 mm/sec was applied to the specimen to maintain the load nearly constantly. In the first and the second weldings, no filler metal was used and both surfaces of the specimen were protected with Ar gas. The welding condition is shown at the top part in **Table 2**. On the other hand,

Table 2 Welding conditions used

Testing Method	Welding method	Current	Voltage	Welding speed	Remark
Cross-bead cracking test	GTAW	55 (A)	9-11 (V)	100 (mm/min)	1.5mmt
Hot ductility test	GTAW	100-105 (A)	11-13 (V)	100 (mm/min)	3mmt
	Pulsed GTAW	I_p=260 (A)* I_b= 10 (A) (I_{av}=72.5 (A))	-	100 (mm/min)	3mmt 12.5Hz
	EBW	30 (mA)	150 (kV)	2000 (mm/min)	3mmt

* I_p: peak current, I_b: base current, I_{av}: average current

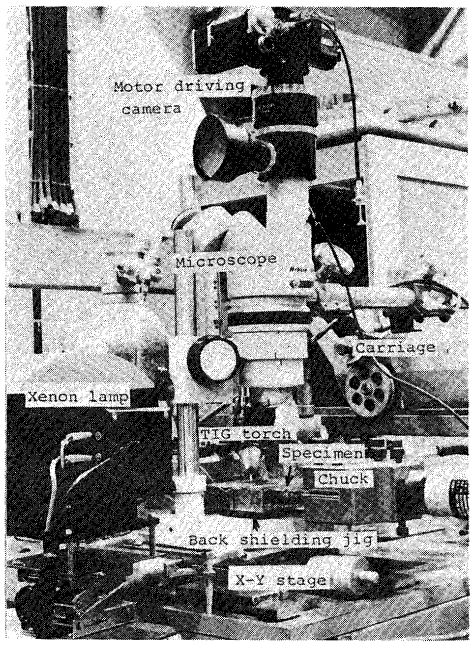

Fig. 2 Apparatus for the MISO technique with the Cross-bead tensile hot cracking test.

dynamic photographing by 35 mm motor-driving camera mounted on a stereomicroscope set above the specimen was done during the test welding. The magnification of film was about 3 times. The apparatus for the MISO technique in the tensile hot cracking test is shown in **Fig. 2**. By the way, it is said[6] that the cracking tendency among different Invars in the Cross-bead tensile hot cracking test under the condition of 15 kgf/mm^2 agrees with that in the self-restraint cracking test.

2.3 Hot ductility test

The configuration of the specimen used in the hot

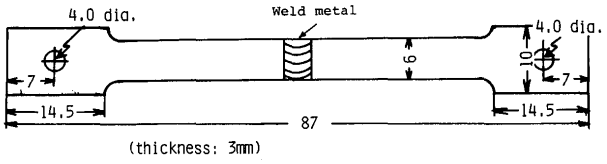

Fig. 3 Specimen configuration used for the hot ductility test.

ductility test is shown in **Fig. 3**, where weld metal was located in the middle of the specimen and tensile deformation was applied perpendicularly to the welding direction. In order to study the effect of weld heat input on the ductility, three welding methods, namely conventional GTAW, pulsed GTAW and electron beam welding (EBW), were used under the condition given in Table 2. The pulsed GTAW was used to get a fully penetrated bead under relatively little heat input.

The specimen was set to a tensile tester coupled with high frequency induction heating system, and was heated in Ar atmosphere. In many hot ductility tests concerning the evaluation of weld hot cracking, tensile deformation is generally applied on a cooling stage after heating up to nil-ductility temperature near melting point. As mentioned later, however, the initiation of the hot crack in the reheated weld metal of Invar in the Cross-bead tensile hot cracking test occurred on a heating stage near peak temperature during weld thermal cycle. Therefore, the tensile deformation was applied on a heating stage in this study, the detailed program of which is shown in **Fig. 4.**

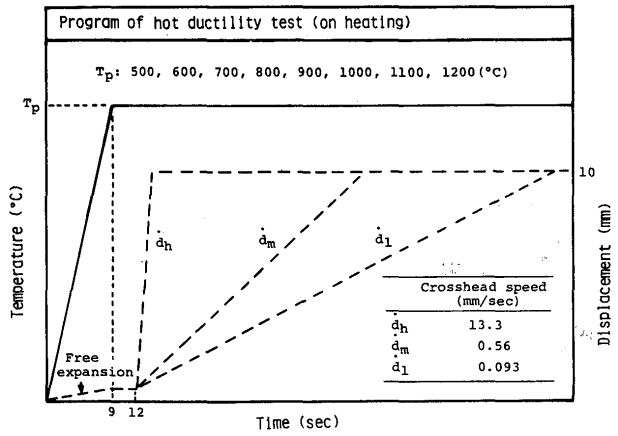

Fig. 4 Program of the hot ductility test.

The heating time from the room temperature to the testing temperature or the peak temperature (T_p) was set to 9 sec, corresponding nearly to the actual GTAW in the cracking test. During the heating, the specimen was allowed to expand freely. The peak temperature selected was 500 to 1200°C at interval of 100°C. Tensile deformation was applied in three kinds of crosshead speed (C.H.S.), namely $\dot{d}_h$, $\dot{d}_m$ and $\dot{d}_l$. The $\dot{d}_h$(13.3 mm/sec) was the highest speed in the tester used, the $\dot{d}_l$ (0.093 mm/sec) was roughly the same as the C.H.S. in the Cross-bead tensile hot cracking test, and the $\dot{d}_m$ was nearly the middle between the $\dot{d}_h$ and the $\dot{d}_l$. The maximum tensile displacement used was 10 mm which was allowable limit in the tester.

Ductility was evaluated by the ratio of reduction in the width after the hot ductility test to the original width, and is represented as $\Delta W/W \times 100(\%)$ hereafter, where ΔW is the reduction of the width and W is the original width.

3. Experimental Results and Discussions

3.1 Dynamic behavior of reheat hot cracking revealed by the MISO technique

An example of the sequence of films by means of the MISO coupled with the Cross-bead tensile hot cracking test is shown in **Fig. 5**. The time, when the tungsten electrode in GTAW torch reached the place apart 4 mm from the center of the first welding pass, was defined as

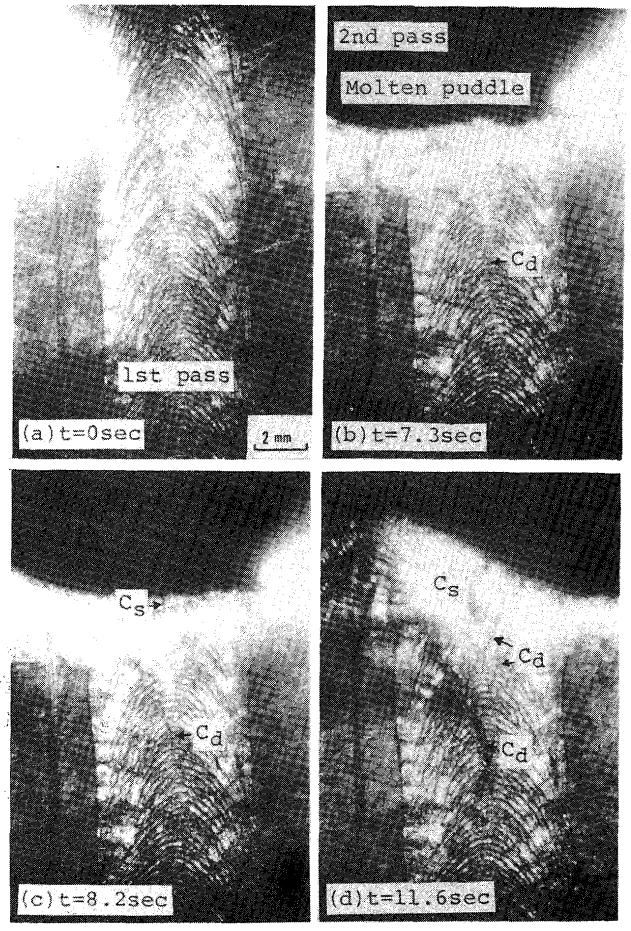

Fig. 5 An example of sequence of films by the MISO technique coupled with the Cross-bead tensile hot cracking test (Item No. of specimen: 12, C_d: ductility-dip crack, C_s: solidification crack).

the starting point, ie t = 0 in Fig. 5(a). The bright zone at the upper left in Fig. 5(a) is arc light and is advancing horizontally to the right. The initiation of reheat hot cracking, namely ductility-dip cracking (C_d), occurred at 7.3 sec in Fig. 5(b) as marked by an arrow. Subsequently the crack propagated to the region of lower and higher temperature as seen in Fig. 5(c) and (d). Moreover, solidification crack (C_s) also occurred in the second welding pass at 8.2 sec as seen in Fig. 5(c), and it was confirmed by scanning electron microscope after the test that this was surely solidification crack from its fractographic feature. At 10.3 sec other ductility-dip cracks (C_d) occurred in the place near the fusion boundary of the second welding pass, perhaps because of strain concentration effect of the solidification crack.

The thermal cycle in the first pass during the second pass welding is shown in **Fig. 6**, where the definition of

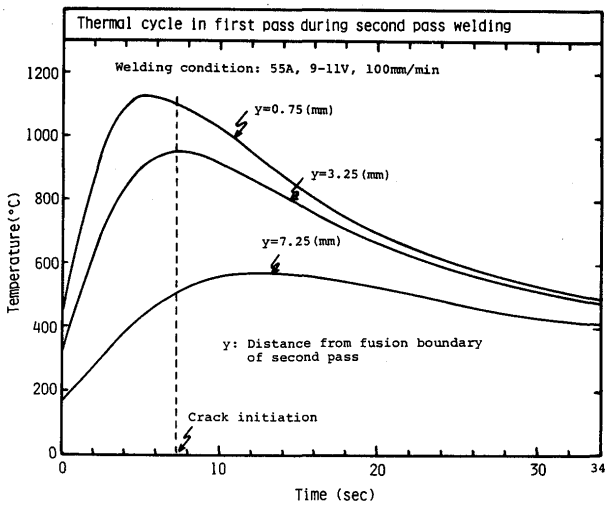

Fig. 6 Thermal cycle in first pass during second pass welding in the Cross-bead tensile hot cracking test.

the starting point of time is the same as that in Fig. 5(a). The mark y means the distance along the first pass from the fusion boundary of the second pass, measured perpendicularly to the welding line of the second pass. As the first ductility-dip crack occurred at 7.3 sec was located at about 4 mm from the fusion boundary of the second pass as seen in Fig. 5(b), it was considered judging from Fig. 6 that the initiation of the ductility-dip crack in the first pass occurred on a heating stage near peak temperature during weld thermal cycle by the second pass.

The thermal cycle in Fig. 6 is converted into temperature distribution shown in the upper part in **Fig. 7**, which is drawn by linear approximation because of relatively little data. Combining the result by detailed film analysis with this temperature distribution, the relation between time lapse and the temperature range of the cracking is given in the lower part in Fig. 7. Figure 7 means: i) The

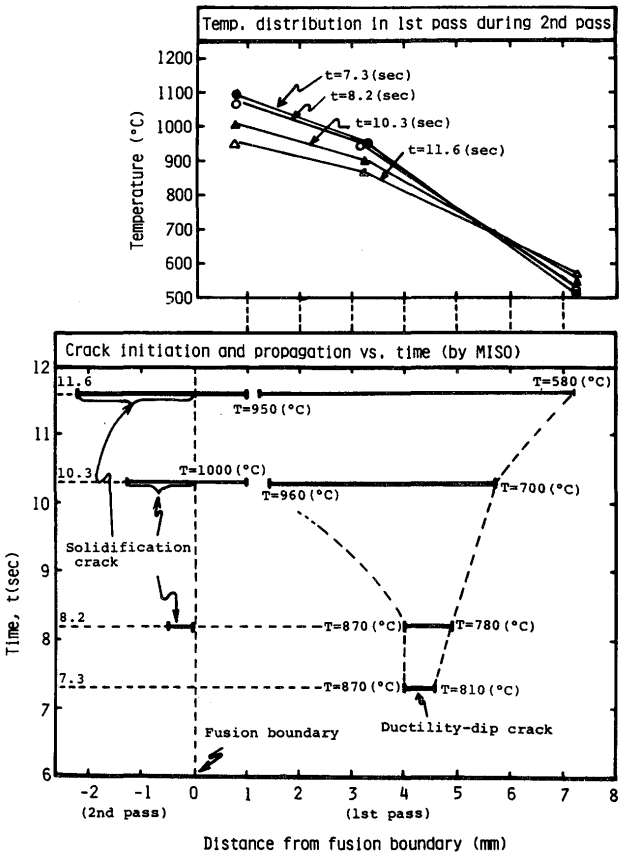

Fig. 7 Behavior of initiation and propagation of ductility-dip cracking revealed by the MISO technique (Item No. of specimen: 12)

initiation of the ductility-dip crack occurred at about 850°C. ii) The crack propagated within the temperature range between about 600 and 1000°C. Although the peak temperature in the first pass at the vicinity of the second pass during the second pass welding is considered to be about 1400°C according to the liquidus temperature of Invar, the crack propagated to this part only when its temperature cooled to about 1000°C. Therefore, it is judged from these results by means of the MISO that the ductility trough causing the crack extends from about 600 to 1000°C and that the minimum ductility is located at about 850°C.

3.2 Characteristics of ductility evaluated with the hot ductility test

3.2.1 Effect of crosshead speed on hot ductility

It has been pointed in the above mentioned that the ductility-dip crack occurs in the temperature range from 600 to 1000°C. So then, the hot ductility test was done from 500 to 1200°C. One of the results is shown in **Fig. 8.** Now the ductility is represented as $\Delta W/W \times 100(\%)$ as mentioned in 2.3. It is seen that there is a low ductility range between about 600 and 1000°C and the ductility

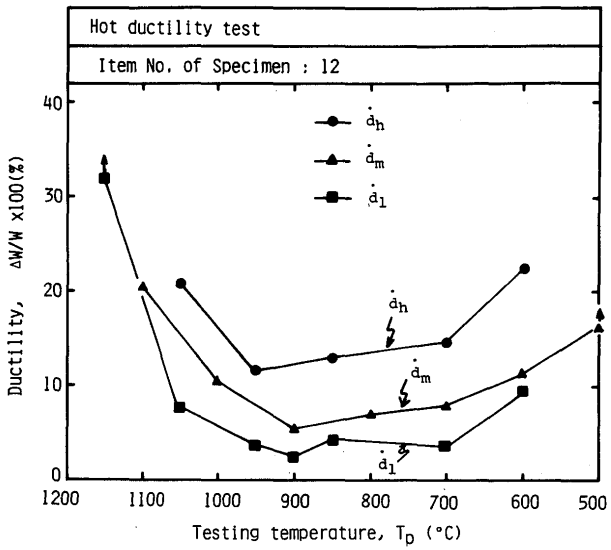

Fig. 8 Typical example of ductility curve evaluated by the hot ductility test.

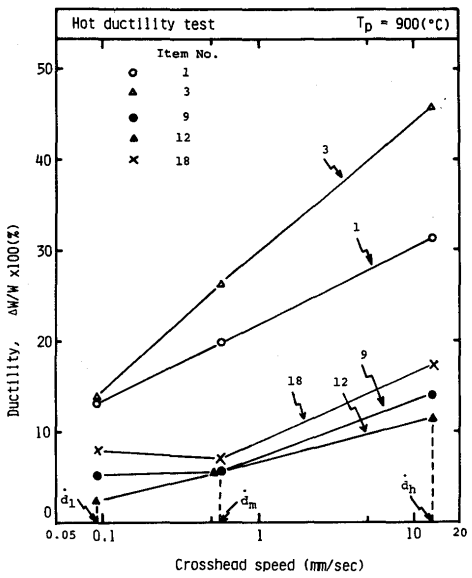

Fig. 9 Effect of crosshead speed on hot ductility at 900°C.

decreases in the order of $\dot{d}_h$, $\dot{d}_m$ and $\dot{d}_l$, where $\dot{d}_l$ is nearly similar to the C.H.S. in the Cross-bead tensile hot cracking test. The minimum of ductility is observed at about 900°C irrespective of C.H.S. Therefore, these characteristics of ductility correspond well to the cracking behavior in the Cross-bead cracking test above mentioned.

Figure 9 shows the effect of C.H.S. on the ductility at 900°C, and it is clearly seen that high C.H.S. causes high ductility. This reason is related to grain boundary sliding as discussed in the next paper[7]. Now the selection of proper C.H.S. is important problem. Of course, C.H.S. should be as slow as possible from the viewpoint of severe test. However, the test under too slow C.H.S. may not be realistic, because weld thermal cycle is rapid. Moreover, high C.H.S. may be recommendable from the viewpoint of experimental efficiency. Concerning this, it is noticed that the difference in ductility between $\dot{d}_l$ and $\dot{d}_m$ is little in the crack-susceptible specimens, namely Item Nos. 9, 12 and 18 in Fig. 9. Moreover, fractographic feature also suggests that $\dot{d}_m$ is available for actual test as explained nextly. The fractographs of the reheat hot crack in the Cross-bead tensile hot cracking test are given in three different magnifications in **Fig. 10**. The fractographs in

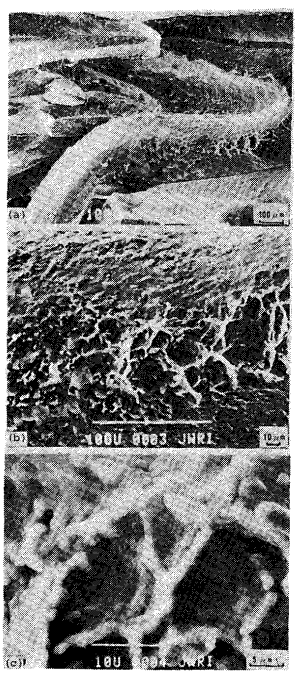

Fig. 10

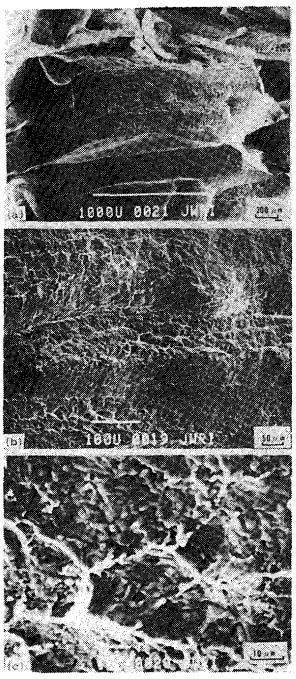

Fig. 11

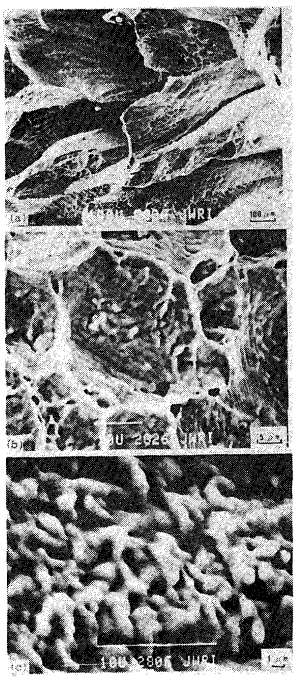

Fig. 12

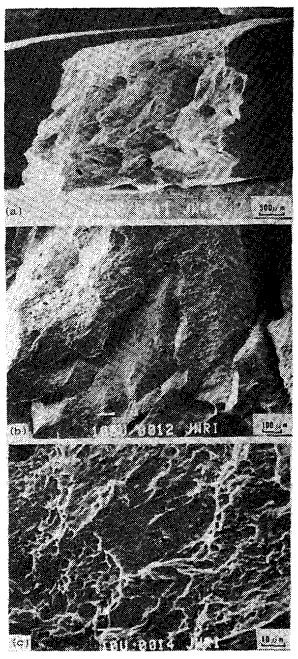

Fig. 13

Fig. 10 Microfractographs of ductility-dip crack in the Cross-bead cracking test
Fig. 11 Microfractographs in the hot ductility test under $\dot{d}_l$.
Fig. 12 Microfractographs in the hot ductility test under $\dot{d}_m$.
Fig. 13 Microfractographs in the hot ductility test under $\dot{d}_h$.

the hot ductility test under $\dot{d}_l$, $\dot{d}_m$ and $\dot{d}_h$ are given in **Figs. 11**, **12** and **13**, respectively. All of the fractographs show a feature of intergranular fracture. Comparison among these means: i) The feature of the fracture surfaces in the hot ductility test under $\dot{d}_l$ is well similar to that in the Cross-bead cracking test even in high magnification. ii) Although there are somewhat more dimples in the hot ductility test under $\dot{d}_m$ than those under $\dot{d}_l$ and in the Cross-bead cracking test, overall feature of the fracture surface under $\dot{d}_m$ is nearly similar to those. iii) The macroscopic fracture mode under $\dot{d}_h$ is shear fracture type in a sense, and many shear dimples are observed on the intergranular fracture surface as seen in Fig. 13. These features are fairly different from that in the Cross-bead cracking test. Therefore, the C.H.S. of $\dot{d}_m$ was selected in the test mentioned later.

3.2.2 Correlation between crack susceptibility and hot ductility

The hot ductility curves of the all testing materials evaluated by $\dot{d}_m$ are shown in **Fig. 14**. The total crack

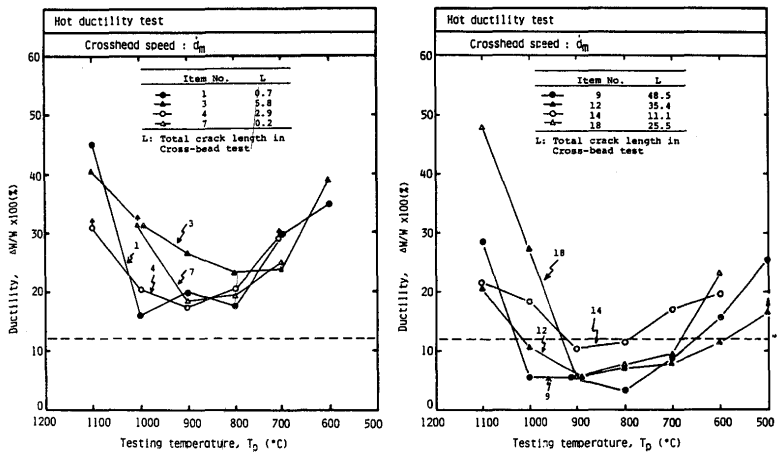

Fig. 14 Summary of ductility curves of all specimens used.

lengths (L) in the Cross-bead tensile hot cracking test are also shown in Fig. 14. Generally the feature of hot ductility curve is simply characterized with two parameters, namely brittleness temperature range (BTR) and the minimum ductility. In order to evaluate BTR, a threshold ductility must be determined, the range under which is defined as BTR. Concerning this problem, the reheat hot cracking in the Cross-bead cracking test occurred in the temperature range from about 600 to 1000°C as shown in Fig. 7, where the item No. of specimen was 12. Now, the threshold ductility, under which the temperature range of ductility curve of item No. 12 extends from about 600 to 1000°C in Fig. 14, is about 12 in $\Delta W/W \times 100(\%)$. Therefore, 12 in $\Delta W/W \times 100(\%)$ was selected as the threshold level, and the all brittleness temperature ranges (ΔT) thus evaluated are compared with the total crack lengths (L) in the Cross-bead cracking test as seen in **Fig. 15**. Generally the increase in ΔT accompanies the increase in L. **Figure 16** giving the correlation between L and the minimum ductility means that the decrease in the minimum ductility also accompanies the increase in L. Now, the left region of the broken line at L = 10 mm in the abscissas in Figs. 15 and 16 is crack-free zone in the actual

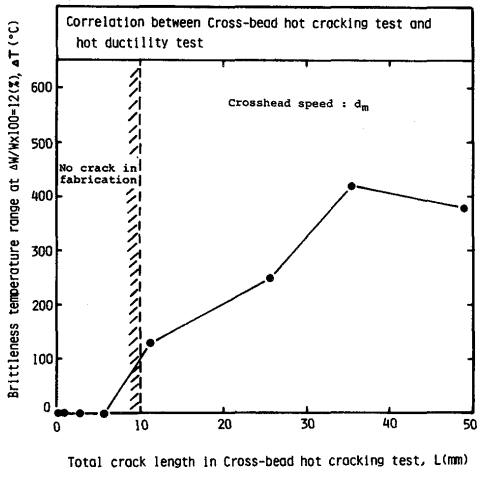

Fig. 15 Correlation between total crack length in the Cross-bead cracking test and brittleness temperature range ΔT.

fabrication of membrane-type model tank[2]. Therefore, ΔT less than about 100°C and/or the minimum ductility higher than about 15% should be attained for crack free material in fabrication.

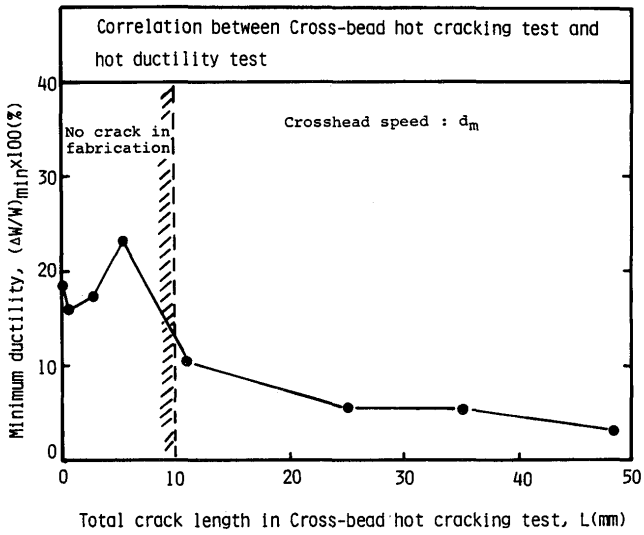

Fig. 16 Correlation between total crack length in the Cross-bead cracking test and the minimum ductility.

3.2.3 Effects of weld heat input and atmospheric gas in hot ductility test on hot ductility

Figure 17 shows the effect of weld heat input on the ductility of reheated weld metal. Pulsed GTAW was used together with the conventional GTAW in order to obtain full penetration through thickness under relatively low heat input. It is seen that low heat input improves the ductility. This effect of low heat input was confirmed in the self-restraint cracking test[8]. The beneficial effect of low heat input may be attributed to small grain size diminishing the grain boundary sliding per one grain boundary.

Figure 18 shows the effect of testing atmosphere on hot ductility, together with the data of EBW and base metal. The letter in bracket in Fig. 18 means the atmosphere in the hot ductility test. It is understood that air

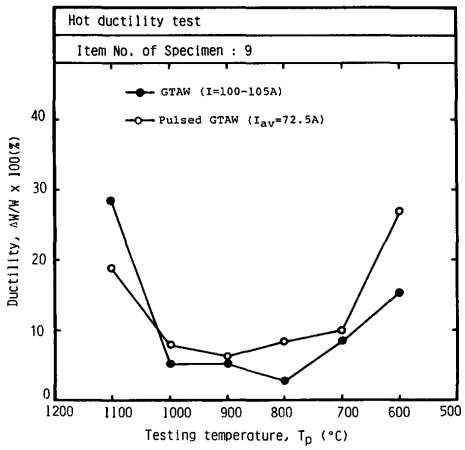

Fig. 17 Effect of weld heat input on ductility curve.

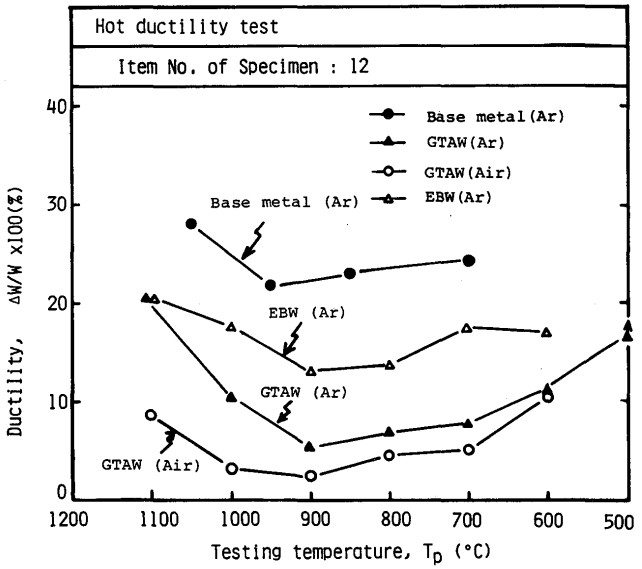

Fig. 18 Effect of weld heat input and atmospheric gas during hot ductility test on ductility

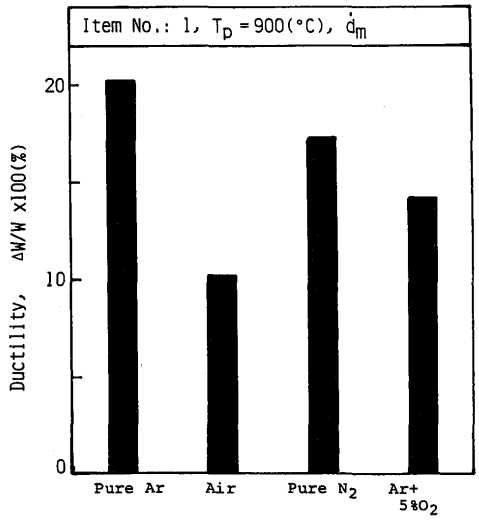

Fig. 19 Effects of air, nitrogen and oxygen gas on ductility.

lowers the ductility, and that EBW gives good ductility. The reason for the high ductility in EBW is perhaps owing to both very low heat input and little gas contamination during welding. **Fig. 19** compares the effects of air, nitrogen and oxygen on the ductility at 900°C in order to study which of nitrogen and oxygen in air is harmful, and means both nitrogen and oxygen are harmful. It is interesting to say that both are crack-promoting element according to the regression analysis in the previous paper[2]. Oxygen in atmosphere maybe lowers the ductility in the same manner as grain boundary oxidation in Ni-base super alloys[9].

These mean that attention should be paid concerning the selection of weld heat input and protection of weld metal from atmosphere in actual fabrication.

4. Conclusions

The direct observation technique MISO coupled with the Cross-bead tensile hot cracking test and the hot ductility test were utilized to analyze the feature of the hot crack in reheated weld metal of Invar. Main conclusions obtained are as follows:

1) The MISO technique proved that the initiation of the reheat hot cracking occurs at about 850°C and the propagation does in the temperature range from about 600 to 1000°C in the Cross-bead cracking test. This behavior has good correlation with the ductility trough evaluated with the hot ductility test.
2) Increase in the crosshead speed in the hot ductility test generally causes high ductility and different fracture mode from that in the weld cracking test. Judging from the ductility and the fracture mode, the crosshead speed of 0.56 mm/sec was utilized as proper one. The ductility characteristics evaluated by the crosshead speed of 0.56 mm/sec had a good correlation with the crack susceptibility obtained in the weld cracking test.
3) Hot ductility which secures crack-free welding in fabrication of membrane-type LNG tank was recommended from the viewpoint of brittleness temperature range and the minimum ductility. Namely, brittleness temperature range less than about 100°C and/or the minimum ductility higher than about 15% should be attained for crack-free material in fabrication.
4) Increase in weld heat input and atmospheric gas contamination lowered hot ductility. Therefore, attention should be paid about welding conditions and welding atmosphere.

Acknowledgement

The authors would like to thank Kawasaki Steel Corp. for the offering of materials used, Hitachi Zosen Corp. for the execution of EBW, and Mr. A. Ariyoshi who was the student of Kinki University for his cooperation in this study.

References

1) H. Nakagawa, et al: Trans. JWRI, Vol.9 (1980), No.2, p.197.
2) F. Matsuda, et al: Trans. JWRI, Vol.13 (1984), No.2, p.241.
3) F. Matsuda, et al: Trans. JWRI, Vol.7 (1978), No.1, p.59.
4) F. Matsuda, et al: Trans. JWRI, Vol.12 (1983), No.1, p.65.
5) F. Matsuda, et al: Trans. JWRI, Vol.12 (1983), No.1, p.73.
6) K. Osaki: Private Communication
7) to be published
8) to be published
9) K. Mino, et al: J. Japan Inst. Met. Vol.44 (1980), No.12, p.1397 (in Japanese).